Proposal for PhD topic: Two Neutron Correlation Study in Photofission of Actinides

Roman Shapovalov

Physics Department at
Idaho State Univerdity

Adviser: Prof. Dan Dale

October 19, 2011

Abstract

It is well known that two fission fragments (FF's) are emitted essentially back to back in the laboratory frame. That can be used widely in many applications as a unique signature of fissionable materials. However, such fission fragments are difficult to detect. The energy and angular distributions of neutrons, on the other hand, are easy to measure, and that distribution will carry information about the fission fragments energy and angular spectra, as well as the neutron spectra in the fission fragment rest frame.

We propose to investigate the two neutron correlation yield resulting from two FF's as a function of different targets, the angle between the two neutrons and the neutron energies. The preliminary calculation of the two neutron correlation shows a huge asymmetry effect: many more neutrons are emitted anti-parallel to each other than parallel to each other. That asymmetry becomes even more if the energy cut on each neutron is done. This study will potentially permit a new technique for actinide detection for homeland security and safeguards applications as well as improve our knowledge of correlated neutron emission.

Contents

Chapter 1

Statement of the physics problems

1.1 Simple summary of fission physics

The physics of photofission is well described in many books [1, 2]. The overall process can be schematically represented as shown in Fig. 1.1. What we are going to discuss here is up to the time scale of about $10^{-14} - 10^{-13}$ sec when the prompt neutrons are emitted from the fully accelerated fragments and completely ignore all the following processes where the prompt gammas and delayed β, γ and n are emitted We will only touch on some specific information we will need to understand the underlying physics in the proposed two neutron correlational study. That mechanism is, of course, in some sense, an approximation, because we do not count possible "scission" neutrons emitted at the instant of fission [10]. What we assume here is that all neutrons are emitted from fully accelerated fission fragments.

It has long been known that the photofission reaction with a heavy nucleus in the energy range of the giant dipole resonance goes through the intermediate compound nucleus. That intermediate nucleus is in an excited state followed by the emission of two fission fragments:

$$\gamma + A \rightarrow A^* \rightarrow FF_1 + FF_2 + TKE \tag{1.1}$$

where TKE is the total kinetic energy which will be shared by the two fission fragments. In general, the TKE will be a function of the fragment mass which has been measured by several authors [19, 20, 21, 22] as seen in Fig. 1.2. Because the fission fragments are essentially non relativistic, the TKE will be distributed proportional to their mass ratio as:

$$\frac{T_1}{T_2} = \frac{M_2}{M_1} \tag{1.2}$$

where T_1, T_2 are the kinetic energies of fragments 1 and 2 such that $TKE = T_1 + T_2$ and M_1, M_2 are their rest masses correspondingly.

The typical mass distribution at the energy range not too far from the threshold barrier is shown in Fig. 1.3 [14]. It is symmetric about $A = 120$ and for every heavy fragments there is a corresponding light one, but the fission with two equal mass fragments is less probable by a factor of about 200. It is interesting, that as the energy of incident γ's increases, the masses of two FF's tend to be equal [15].

The angular distribution of individual FF's can be explained according to A.Bohr's fission channel concept [5] and briefly described by R.Ratzek et al. [11] with regards to photoinduced

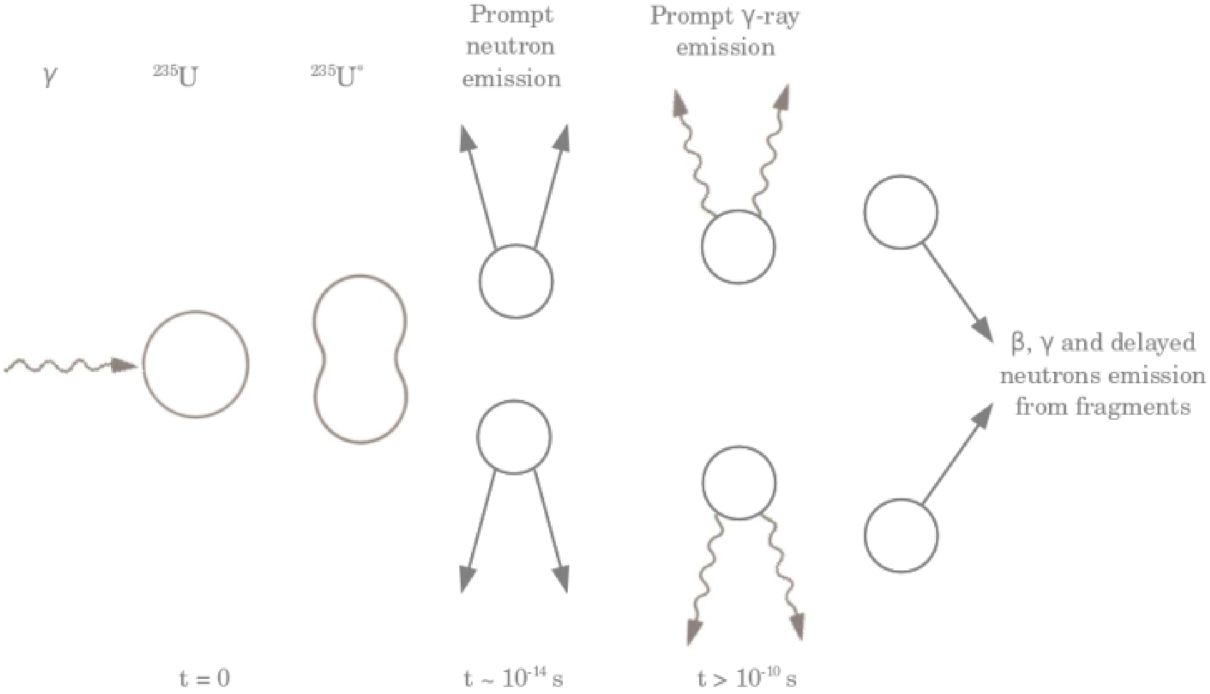

Figure 1.1: Schematic representation of the fission process in uranium. Neutrons are emitted from fully accelerated fission fragments. The time scale gives the orders of magnitude only.

reactions. If we restrict ourselves to the photofission of an even-even nucleus ($J^{\pi} = 0^{+}$, such as ^{238}U) and consider only electric dipole (E1) transactions, the angular distribution of fission fragments can be written as [11]:

$$W(\Theta) = A_0 + A_2 P_2(cos\Theta) \tag{1.3}$$

The angular distribution coefficients A_0 and A_2 depend on the transition state (J,K), where K is the projection of the total spin J on the symmetry axis of the deformed nucleus. For J = 1, K = 0, we have $A_0 = \frac{1}{2}$, $A_2 = -\frac{1}{2}$ and for J = 1, K = 1, we have $A_0 = \frac{1}{2}$, $A_2 = \frac{1}{4}$. $P_2(cos\Theta) = \frac{1}{2}(2 - 3\sin^2\Theta)$ is the Legendre polynomial. Qualitatively, the angular distribution of the fission fragments can be explained if we consider the nuclear excitation as a collective motion of neutrons against the protons [4]. Because the incident gammas are a transverse wave, that will cause protons to oscillate against the neutrons in the direction of electric field **E** followed by the splitting of nucleus into the two fission fragments.

Some simple considerations of kinematic of reaction 1.1 can clarify some important moments. In the first step the incident gammas interact with heavy nucleus A resulting in compound intermediate state A*. For such a step, if the energy of incident gammas is small, say below or about 20 MeV, after applying the momentum conservation law, we can easily see that the excited nucleus A* is almost in rest. Because of that, and applying the momentum conservation law to the last step of reaction, we conclude that the two FF's are flying away almost in opposite direction as seen in the laboratory frame. This simple conclusion is very important and can be used widely in many applications as a unique signature of fissionable materials.

After about $10^{-14} - 10^{-13}$ sec the fission fragments will emit neutrons. As was already

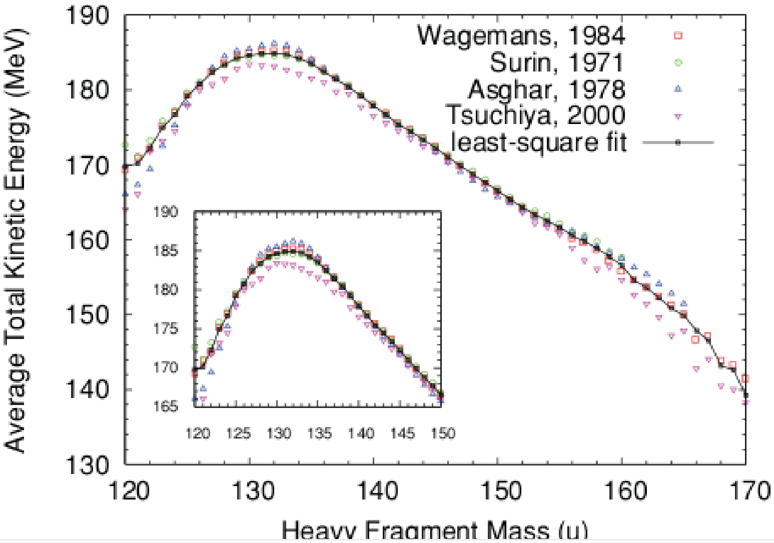

Figure 1.2: The average TKE as a function of the heavy fragment mass. The solid line is the result of a least-square fitting of the experimental data sets.

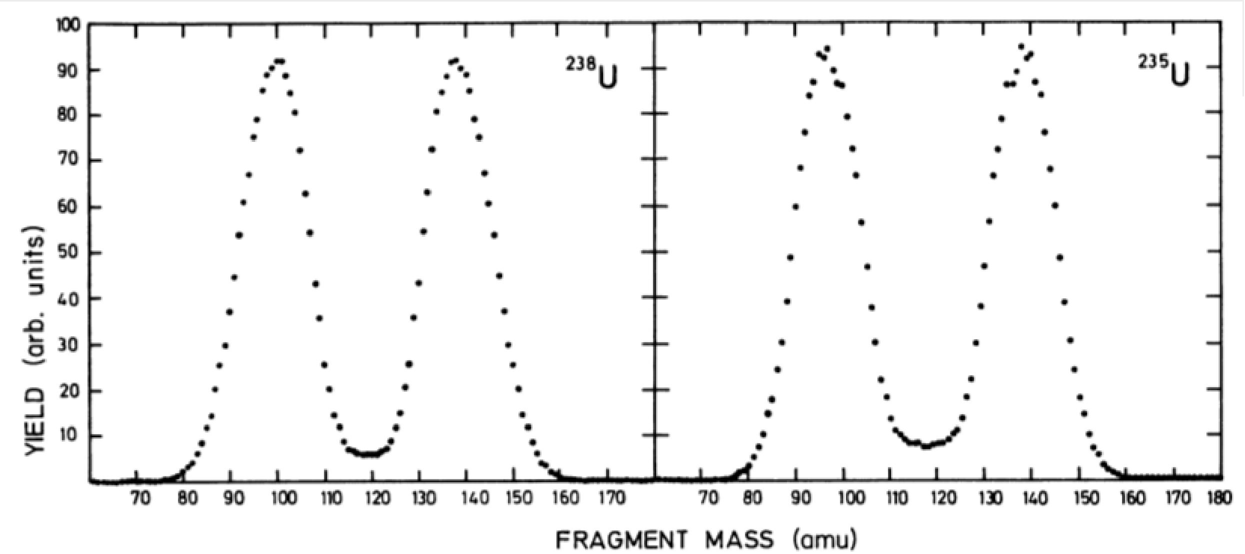

Figure 1.3: Integrated fission fragments yield (arbitrary units) versus fragment mass for the photofission of ^{238}U and ^{235}U with 25-MeV bremsstrahlung

mentioned, it was assumed that all prompt neutrons are emitted from fully accelerated fragments, and there are no so called "scission" neutrons emitted at the time of fission. The important parameter to be considered here is the total excitation energy (TXE) of the intermediate nucleus A^*. That total excitation energy will be shared among light and heavy fragments, and the exact form of such distribution is the open question. However, there is strong evidence [23, 24] that when the excitation energy is relatively low the light fragments will acquire the larger part of that shared energy. Those excited fission fragments can release energy and angular momentum by emitting prompt neutrons and prompt γ rays as well, but it can be assumed that the initial energy release is completely due to the neutron emission [17]. Because the excitation energy of the fission fragments is large in comparison with the lowest lying nuclear levels, the statistical model to analyze the neutron emission spectrum can be applied [3]. Using that approach, to a very good approximation, the angular distribution of prompt neutrons is isotropic in the center-of-mass frame of the fission fragments. The energy of the evaporated neutrons can be described by the Maxwell distribution with the spectrum temperature T:

$$\rho(\epsilon_n) = \epsilon_n \exp\left(\frac{\epsilon_n}{T}\right) \tag{1.4}$$

where ϵ_n is the neutron kinetic energy in the center-of-mass fragment frame.

After the first neutron is emitted the second one will be emitted and so on until the excitation energy of the fragments becomes less then the neutron separation energy. Finally, the rest of the excitation energy can be released by prompt γ ray emission. However, what we assume here is that only one neutron is emitted from the fully accelerated fission fragments.

Below is a short summary of the photofission reaction mechanisms discussed above which will be used in the following section to discuss the idea of the proposed two neutron correlation:

- two fission fragments recoil essentially back to back.
- the angular distribution of the prompt neutrons is isotropic in the center-of-mass frame of the fission fragments with a statistical energy distribution.
- each fully accelerated FF emits only one neutron.

1.2 Idea of 2n correlations

Let's start to count how many FF's pairs are going antiparallel and how many FF's pairs are going parallel to each other. Because two fission fragments recoil back to back, the FF's asymmetry would be, of course, infinity (there are no two FF's going parallel to each other):

$$\mathrm{A_{FF}} = \frac{\mathrm{FF's\ antiparallel}}{\mathrm{FF's\ parallel}} = \infty \tag{1.5}$$

where *FF's antiparallel* is the number of FF's pairs going in antiparallel direction and *FF's parallel* is the number of FF's pairs going in parallel direction.

The problem here is that fission fragments are very difficult to detect. For a target thicker than a few mg/cm^2, due to their heavy ionization loss, almost all fission fragments will stop their path inside the target. On the other hand the neutrons emitted by these fission fragments will fly outside of the target and could be easily detected. The question here is whether or not the angular asymmetry of fission fragments (they are always back to back) is manifest in the angular distribution of prompt neutrons. In order to answer this, we propose to measure the two neutrons angular and energy distributions with the ultimate goal of calculation the two neutron asymmetry:

$$\mathrm{A_{2n}} = \frac{\mathrm{2n's\ antiparallel}}{\mathrm{2n's\ parallel}} \tag{1.6}$$

where *2n's antiparallel* is the number of 2n's pairs going in antiparallel direction and *2n's parallel* is the number of 2n's pairs going in parallel direction as seen in the LAB frame.

If we take a typical 1 MeV neutron in the center-of-mass frame of the fission fragment it will travel with the speed of about 4.6% of the speed of light. The angular distribution of neutrons in this frame will be essentially isotropic as was discussed previously. If we take two fission fragments with typical mass numbers $A_1 = 95$ and $A_2 = 143$ they will travel with the speed of about 4.6% and 3.0% of the speed of light correspondingly, and they will fly away in the opposite direction. The energy and angular distribution of neutrons observed in a LAB frame will be a superposition of these two spectra: 1) the spectrum of neutrons in the fission fragment rest frame and 2) the spectrum of the fission fragments.

The expected 2n correlation asymmetry could be thought of as a product of asymmetry of two fission fragments $\mathrm{A_{FF}}$ (f-la 1.5) times a washing effect due to isotropic angular distribution of neutrons in the fission fragment rest frame $\mathrm{W_n}$ times a washing effect due to multiple Coulomb scattering inside the target and surrounding materials $\mathrm{W_{scat}}$:

$$\mathrm{A_{2n}} = \mathrm{A_{FF}} \cdot \mathrm{W_n} \cdot \mathrm{W_{scat}} \tag{1.7}$$

Because the first term is a large we can expect that the total two neutrons asymmetry as measured in laboratory frame (f-la 1.6) would be the sufficient to observe.

Chapter 2

Brief review of what has been done

The first ever measurements of photofission fragments' angular distribution were performed on Thorium in 1952 - 1954 by several authors [6, 7, 8] and were summarized and briefly discussed by Winhold and Halpern in 1956 [9]. It was found that the observed angular distribution has the form $a + b\sin^2\Theta$ (Fig.2.1) and the ratio b/a depends on the energy of the photons producing the fission, on the particular fissionable target being irradiated, and on the particular fission fragments being observed. Itwas found that the photons in the giant resonance region produce essentially isotropic fission and the anisotropic fission is due solely

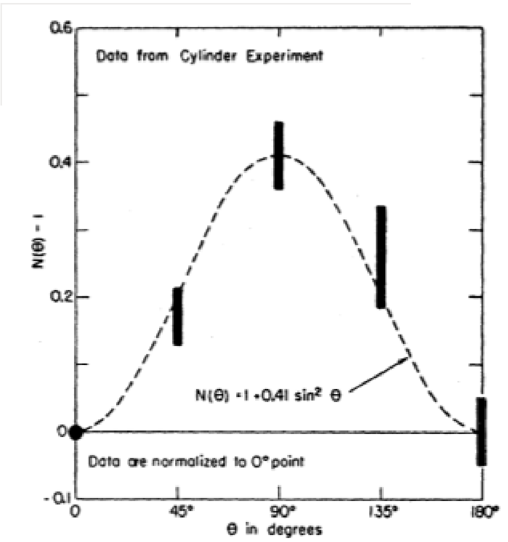

Figure 2.1: The angular distribution, $N(\Theta)$, of fission fragments from Th^{232} caught at the angles Θ to the x-ray beam. The x-ray beam was produced in a thick lead target by an electron beam whose spectrum was centered at 13 MeV and was about 5 MeV wide.

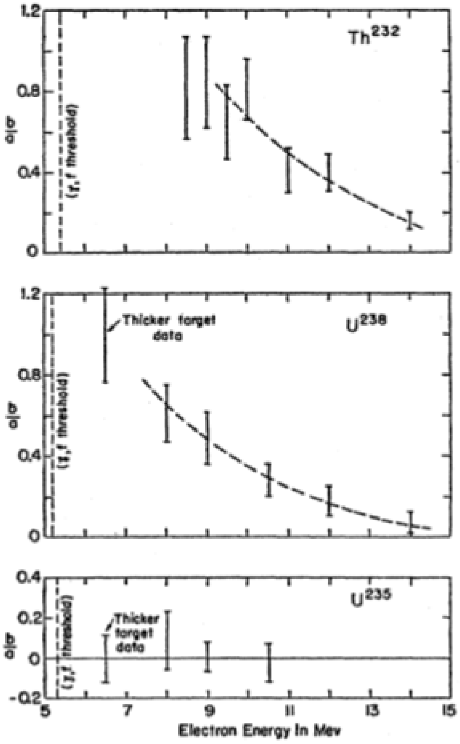

Figure 2.2: The anisotropy in the photofission of three targets. The angular distributions were all assumed to be the form $a + b\sin^2\Theta$.

to photons with in about 3 MeV of the fission threshold. As can been seen from Fig 2.2 the anisotropies in Th^{232} and U^{238} decrease rapidly with increasing electron energy and there are not any anisotropies for U^{235} was measured. That was discussed and analyzed using the Bohr model of collective motion [5].

Years later in 1962 the neutron angular and energy distributions were measured by Bowman et all [10]. They analyzed the spontaneous fission of ^{252}Cf by using the time of flight technique to measure the neutron angular and energy distributions in coincident with the fission fragments. The experimental data was analyzed by assumption that there are no 'scission' neutrons and there are 10% of 'scission' neutrons. The last assumption in general gives better agreement with the measured data as can been seen from the Fig. 2.3. The calculated energy spectrum of neutrons in the CM frame is presented in Fig 2.4. The large dots represent the neutrons emitted in the direction of the light fragments and the triangles represent the neutrons emitted in the direction of the heavy fragments. The smaller dots were obtained from measured neutrons emitted in the backward direction from the light fragments. The curve for light fragments was reduced by the factor 1.16, which is the ratio of the number of neutrons from the light fragments to the number from the heavy fragments. The results can be explained well by assumption of isotropic evaporation of neutrons from the fully accelerated fragments.

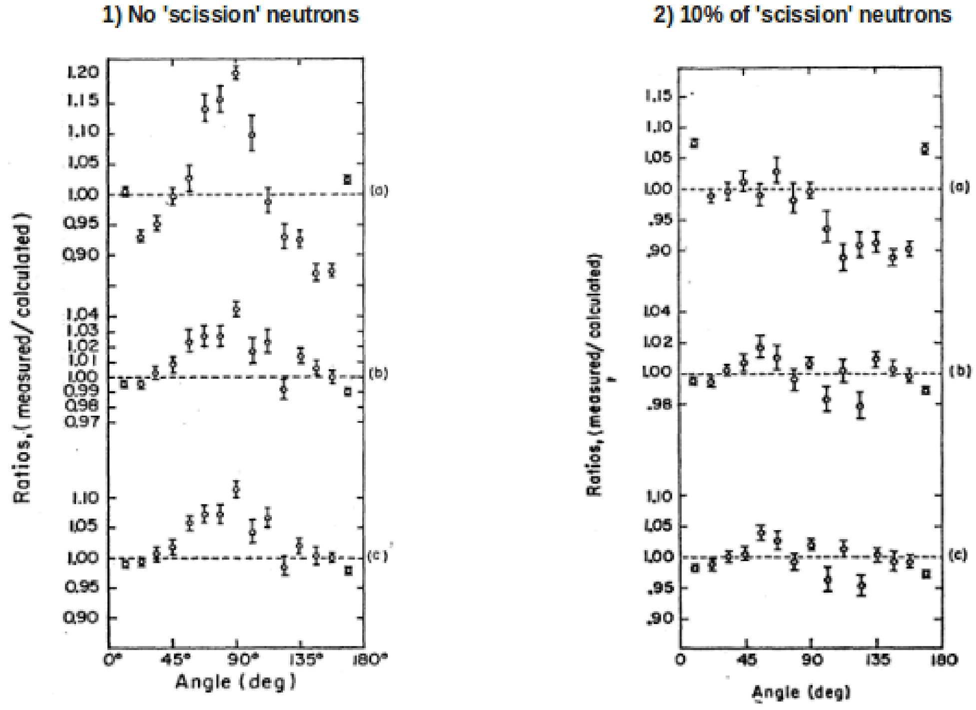

1) No 'scission' neutrons

2) 10% of 'scission' neutrons

Figure 2.3: The ratio of measured to calculated values for (a) numbers of neutrons (b) average velocities, and (c) average energies as a function of angles.

Further measurements of angular and energy distributions of fission fragments and neutrons from the spontaneous fission of ^{252}Cf were made by Budtz-Jorgensen and Knitter in 1988 [12]. The measured neutron energy spectrum (Fig. 2.5) is in very good agreement with the Maxwell distribution in the energy range below 20 MeV energy point with the temperature parameter of $T = 1.41 \pm 0.03$ MeV. The neutron angular distribution recalculated

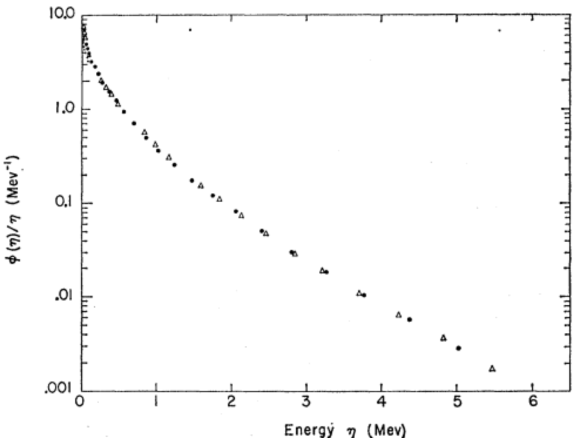

Figure 2.4: The center-of-mass neutron energy spectrum $\phi(\eta)$ (CM) divided by η.

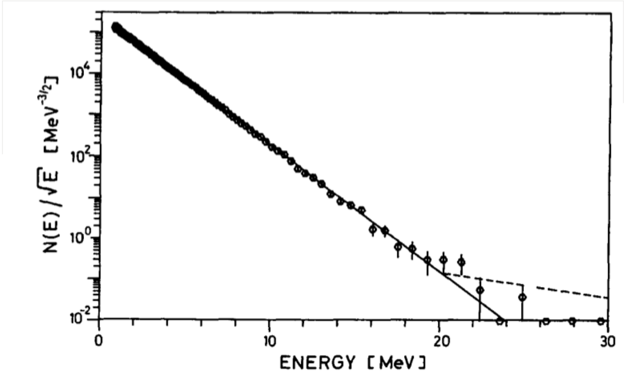

Figure 2.5: Fission neutron energy spectrum divided by the square root of the neutron energy versus the neutron energy. The solid line is Maxwell energy distribution.

in the fission fragment rest frame integrated over all neutron energies and normalized to unity is plotted in Fig. 2.6. The results confirm the isotropic neutrons' angular distribution suggested by many authors in most modern theoretical models. The obtained angular anisotropies are compared by authors with data obtained by Bowman et all [10] as a function of fission neutron energy and is presented in Fig. 2.7. There is good agreement between both measurements up to about 4 MeV and significant discrepancy above that point. The solid line is a theoretical line calculated with the assumption that there are no 'scission' neutrons and is in good agreement with the Budtz-Jorgensen measurements.

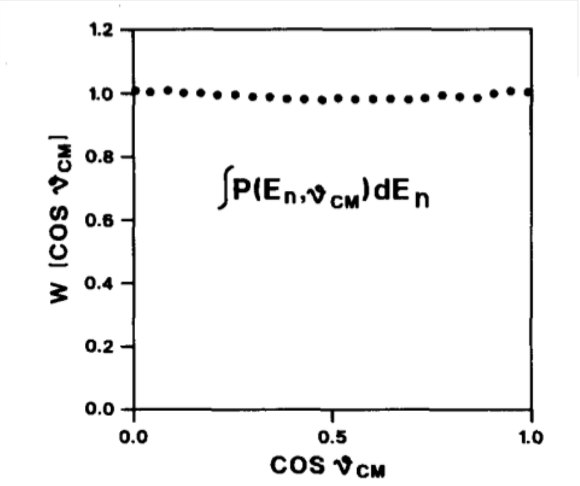

Figure 2.6: Fission neutron angular distribution in the fragment center-of-mass system integrated over all neutron energies

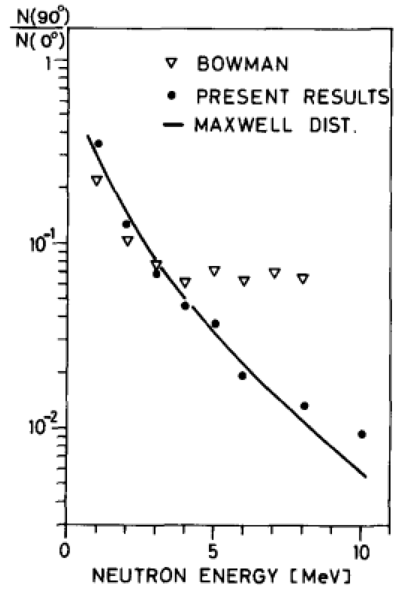

Figure 2.7: Fission neutron intensity ratio $N(90^o)/N(0^o)$ is plotted versus the fission neutron energy.

Chapter 3

Our experimental set-up

We plan to use the HRRL LINAC to construct the beamline to produce the Bremsstrahlung photons. From Dr. Kim's talk, that machine can supply the 20 ns and higher pulse width with about 10-80 mA peak current. That will give to us the freedom to adjust the beam parameters to satisfy the desired condition to have the one fission per pulse as will be described in the following section. Because such a low rate is needed the main advantage of HRRL LINAC is, of course, the hight repetition beam pulse rate of 1000 Hz that will permit to increase the statistics as compared with the other machines available in IAC.

The production of unpolarized photons is a well known technique and is widely described in the literature [13]. When electrons strike the thin radiator, that results in the Bremsstrahlung radiation in the forward with respect to the beam direction. The typical energy spectrum of Bremsstrahlung photons for the 7 MeV endpoint energy is shown in Fig 4.6.

Such beamline of unpolarized photons will be used to measure the two neutrons correlation yield as a function of different targets, the angle between two neutrons and the neutron energy. The time of flight (TOF) technique will be used to identify neutrons and to measure their energy, with the start signal coming from the accelerator beam pulse. A typical 1 MeV neutron travels of about 5% of the speed of flight. If we take the neutron detector located 1 m away from the target, that will correspond to the TOF equal to:

$$\frac{1\ m}{0.05 \times 3 \cdot 10^8\ m/s} \approx 67\ ns$$

The TOF of gammas scattered from the target and flying with the speed of light c will be around 3.3 ns. That will allow to distinguish neutrons from gammas. Fig. 3.1 shows the typical time of flight spectrum from photodisintegration of deuteron measured from previous HRRL runs. By converting the measured time of flight of neutrons to their velocity we will be able to reconstruct the neutron energy. Of course, the error in neutron energy will depend on the LINAC pulse width. For HRRL the minimum pulse width, as was mentioned above, is about 20 ns and that will limit the precision with which we will be able to measure the neutron energy. To reduce such a kind of error the distance from target to detector could be increased up to about 2 m.

Because the one fission per pulse condition is required, the neutron detectors with the big front area are needed. We currently have 16 plastic scintillators with the size of about

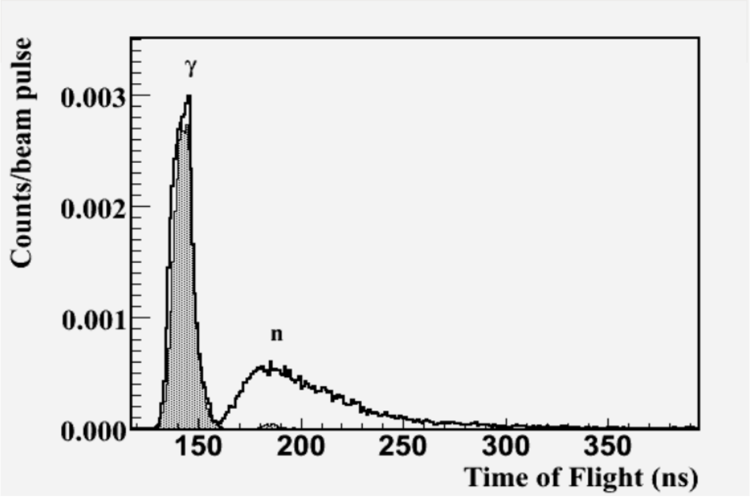

Figure 3.1: Typical TOF spectrum from photodisintegration of deuteron measured from previous HRRL runs. The distance from target to detector is about 2 m. The spectrum illustrate the ability to distinguish gammas peak from neutrons one.

15 cm × 88 cm × 3.8 cm that corresponds to the front area of about 15 cm × 88 cm = 0.132 m^2. As will be shown later for the uranium-238 target, the neutrons are emitted mostly perpendicular to the beam direction (Fig. 4.2). To maximize the 2n correlation yield such plastic scintillators will be placed at the angle of 90 degree with respect to the beam surrounding the target . Further thinking and calculation about the detector location should be done but, in principal, that will allow to almost cover the 2π geometry as can be seen from Fig 3.2. The two PMT will be symmetrically attached to both ends of each detector. To increase the collected light from the detector especially at the area close to the ends, the non-scintillated plastic transparent to the visible and UV light will be placed between the detector and PMT.

Assume the neutron hits the detector at some distance y from the first PMT as shown in Fig 3.3. Two techniques to find the position y can be used here.

The first method is as follows. The amplitudes A_1 and A_2 detected by PMT_1 and PMT_2 correspondingly will be proportional to the distances y and $(l-y)$ that light travels as follows:

$$A_1 = I_0 e^{-\alpha y}$$

$$A_2 = I_0 e^{-\alpha(l-y)}$$

where l is the detector length and α is the attenuation constant. If we take the natural logarithm of the ratio of A_1 and A_2, the distance y where the neutron hit the detector becomes:

$$y = \frac{l}{2} - \frac{1}{2\alpha} \ln \frac{A_1}{A_2} \tag{3.1}$$

The other method we can use here is the timing technique. The TOF T_1 and T_2 detected by PMT_1 and PMT_2 correspondingly can be calculated as follows:

$$T_1 = \frac{L}{c} + \frac{yn}{c}$$

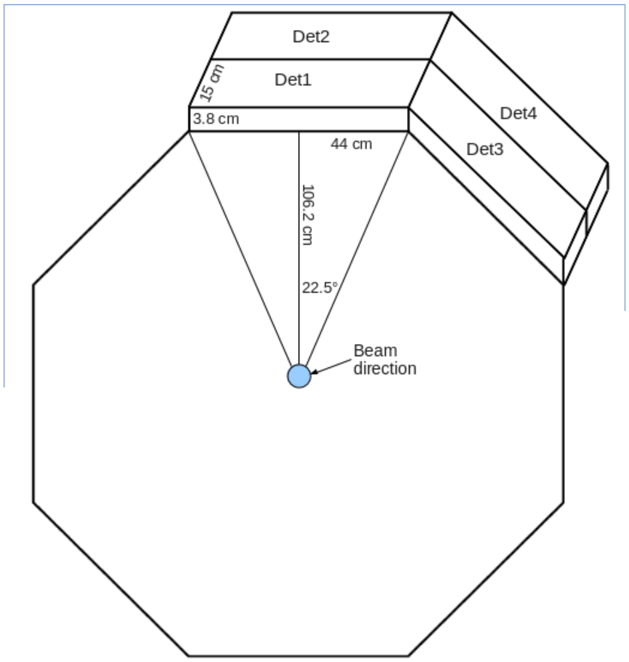

Figure 3.2: Possible detector geometry to measure the two neutron correlation yield. Total 16 neutron detectors are placed at the angle of 90 degree with respect to the beam. The detector size is 15 cm × 88 cm × 3.8 cm.

$$T_2 = \frac{L}{c} + \frac{(l-y)n}{c}$$

where l is as before the detector length, L is a distance the neutron travels from the target to the detector, c is the speed of light and n is the index of reflection of scintillator material used in the detector. Taking the difference of T_1 and T_2 the position y can be found easily:

$$y = \frac{c}{2n}(T_1 - T_2) + \frac{l}{2} \tag{3.2}$$

Both techniques can be used to calculate the position where the neutron hits the detector. However the last method looks more simple and preferable in the following sense. In the first method the amplitudes of both PMT's for each detector should be measured. To find the energy of a neutron, in addition, the TOF spectrum measurements, are needed as well. The two independent channels of an acquisition system are needed in that case for each PMT's. In the last timing technique method the only TOF measurements for each PMT are required. That will allow to find the position y as described by the formula 3.2 as well as the neutron energy by converting the TOF to the neutron velocity. So only one acquisition system channel will be needed in the last case.

Some TOF measurements with 1 PMT attached to the end of the detector and with ^{243}CF source moved along the detector were performed and the results presented in Fig. 3.4. The results show the ability to identify the source position as a function of measured TOF.

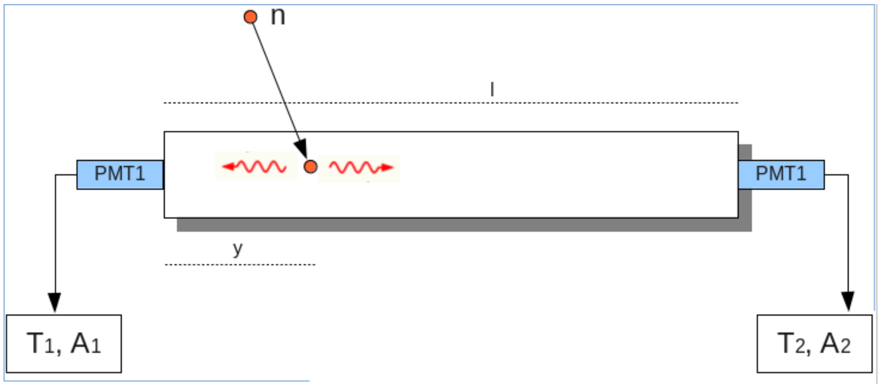

Figure 3.3: Neutron detector with two PMT attached to both ends. Neutron n hits the detector at distance y from first PMT. The amplitude signals A_1, A_2 and TOF signals T_1, T_2 are measured from PMT_1 and PMT_2 correspondingly.

The calculated speed of light inside the scintillator is about 7 cm/sec that corresponds to about $n = 4$ index of reflection. Also note the minimum distance from the source to PMT where the data was collected is about 15 cm. Below that point no signal was detected. That region is a so called 'dead zone' of detector where the light from the scintillator does not go to PMT. To restore this situation some non-scintillated plastic between the end of the detector and PMT as was mentioned above will be placed.

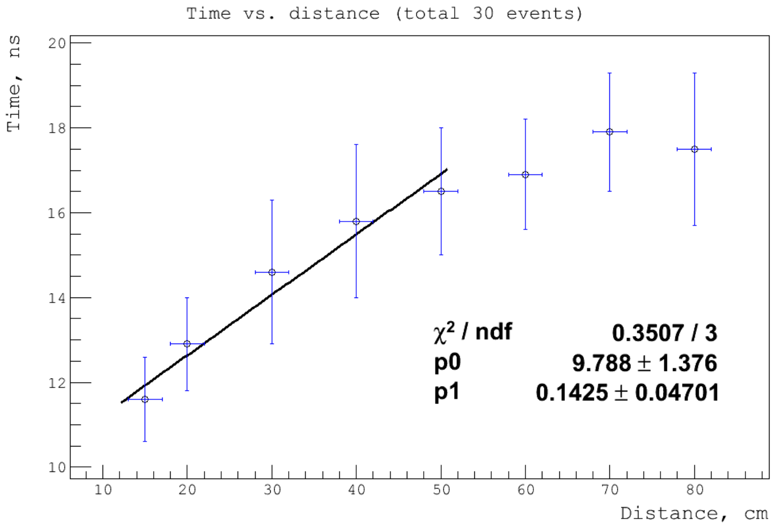

Figure 3.4: TOF measurements with 1 PMT attached to the end of detector and with ^{243}CF source moved along the detector the detector

Chapter 4

Expected results

4.1 Asymmetry calculation

To estimate the expected asymmetry in 2n correlations the Monte-Carlo simulation was performed. A total number of 10 million fission events was simulated. Each neutron was sampled up to 10 MeV in the fission fragment rest frame. The following was assumed here:

- The uranium-238 with $J = 1$ and $K = 1$ is used as the fissionable target.
- The incident gammas are an unpolarized wave.
- The fission fragment mass distribution is sampled uniformly between $85 < A < 105$ and $130 < A < 150$
- A fixed amount of total kinetic energy of 165 MeV is given to the two fission fragments and is distributed between them proportional to their mass ratio
- Each fission fragments emit one neutron. There are total two neutrons, marked as a and b for each fission event. Neutrons are emitted isotropically in the center-of-mass of fully accelerated FF's with the energy distribution given by:

  $$N(E) = \sqrt{E} \exp\left(-\frac{E}{0.75}\right) \tag{4.1}$$

  This reproduces the laboratory neutron energy distribution as measured with (n,f) channel.

- Two recoiled fission fragments emit back to back. Fission fragments angular distribution is sampled according to:

  $$W(\Theta) = \frac{1}{2} + \frac{1}{4}\left(\frac{1}{2}(2 - 3\sin^2\Theta)\right) = \frac{3}{4}\left(1 - \frac{1}{2}\sin^2\Theta\right) \tag{4.2}$$

  for $J = 1$, $K = 1$.

After both angular and energy distributions of neutrons and FF's were sampled using the assumptions above, neutrons were boosted from the fission fragments rest frame into the laboratory frame. The energy and direction of neutrons a and b for every fission event were recorded in the LAB frame.

To be sure that the simulated algorithm is correct, some preliminary results of described above simulations are discussed below.

The energy spectrum of the sum of kinetic energy of two neutrons *a* and *b* emitted by fully accelerated fission fragments as seen in laboratory frame is plotted in Fig. 4.1:

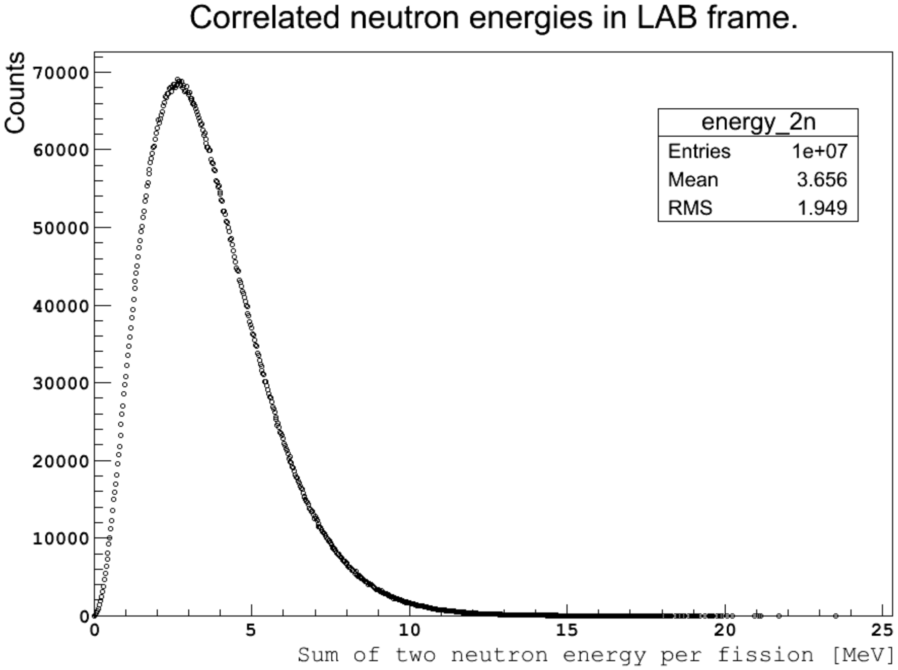

Figure 4.1: The energy distribution of sum of kinetic energy of two neutrons *a* and *b* emitted by fully accelerated fission fragments as seen in laboratory frame

Because the typical neutron energy in the fission fragment rest frame is about 1 MeV and the spectrum above is the spectrum of the sum of two neutron energies, the pick value of about 2.4 MeV looks reasonable after the boost into the LAB frame.

Angular distributions of prompt neutrons, as seen in laboratory frame, are presented in Fig. 4.2. That is, in principal, what everyone should expect for detection of one neutron. Here the neutron *a* is coming from one fission fragment and the neutron *b* is coming from the other one as was assumed above. First we note that angular distributions of both neutrons a and b look statistically similar as we can expect because there are no any reason for discrepancy. Also, as we can see, the resulting angular distribution is strongly anisotropic: more neutrons are emitted in perpendicular to the beam directions ($\cos\Theta = 0$) then those are in parallel ($\cos\Theta = \pm 1$). We can conclude here that the angular distribution of the fission fragments is strongly manifested in the angular distribution of prompt neutrons in laboratory frame. That result is important and could be used widely.

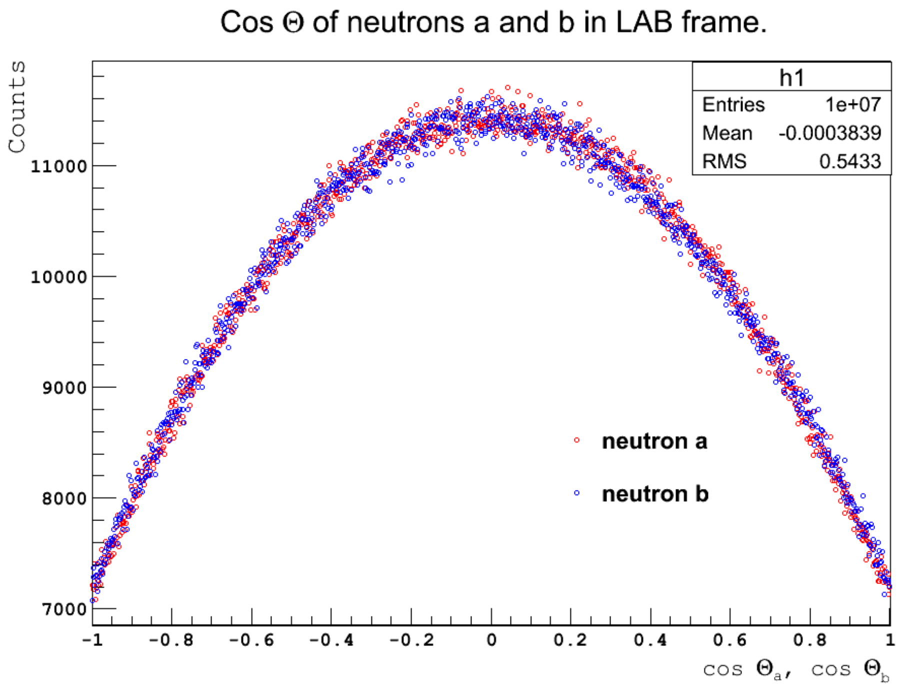

Figure 4.2: Angular distribution of prompt neutrons a (red) and b (blue) emitted by two fission fragments as seen in laboratory frame.

After energy and angular distributions of both neutrons *a* and *b* in the LAB frame were simulated, and we confirmed that our simulation is sensible, the next step is to investigate the two neutron correlation yield as a function of different quantities. We can count, for example, how many of them are going in anti-parallel direction and how many are going in parallel direction with respect to each other. Then the asymmetry in the two neutron correlation can be calculated as (see formula 1.4):

$$\mathrm{A_{2n}} = \frac{\mathrm{2n's\ antiparallel}}{\mathrm{2n's\ parallel}}$$

The results of two neutron correlation as a function of the sum of two neutron energies are represented in Fig. 4.3. Here the following was assumed:

- two neutrons are antiparallel to each other if $\cos(\Theta_{2n}) < -0.9$
- two neutrons are parallel to each other if $\cos(\Theta_{2n}) > 0.9$

where Θ_{2n} is the calculated angle between neutrons a and b as seen in laboratory frame.

Of course, we cannot count events corresponding to the certain neutron energy, or to the sum of two neutron energies. When we are saying that, we are always assuming some energy interval in which events were counted. The exact values of intervals were used and numerical values of calculated 2n asymmetry and different yields are shown in table 4.1.

As we can see the resulting two neutron asymmetry is a strong function of the sum of two neutron energies. It increases from about 2 up to about 80 as we move from 0 to 10

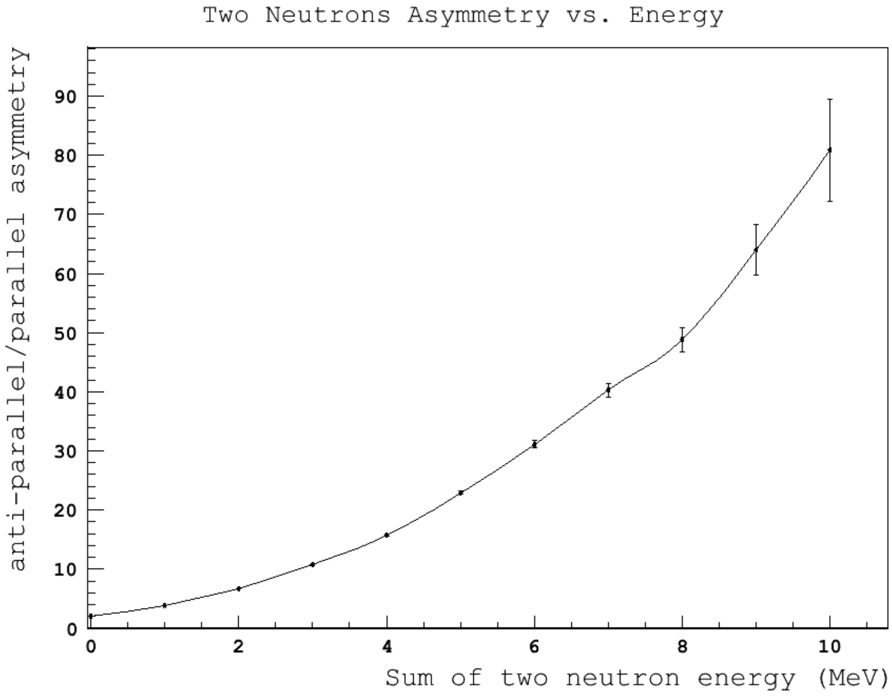

Figure 4.3: Calculated 2n asymmetry (antiparallel/parallel) as a function of the sum of two neutron energies

MeV energy point. Also note, that at the higher energy points the error becomes significant and reaches up to 10% value at the 10 MeV point. That is simple because the number of counts becomes smaller at the higher energy range. As we can see from table 4.1, for example, at 10 MeV energy point the numbers of neutron pairs going in antiparallel and in parallel direction are about 7200 and 90 correspondingly. The asymmetry yield at this point, which we can define as the sum of neutron pairs going in antiparallel and parallel directions divided by the total number of events, is about 0.07%. So, if we would like to study the high asymmetries at the high energy interval, to reduce the error bar a big statistic is needed. The maximum asymmetry yield of about 2.7% is reached at the (3 - 4) MeV energy interval and the corresponding asymmetry is about 10 here. It could be noted that asymmetry yields

Table 4.1: Calculated 2n asymmetry (antiparallel/parallel) as a function of the sum of two neutron energies

#	(Ea+Eb), MeV	cnts_total	cnts_int	cnts180	cnts0	2n Yield	Asymm Yield	Asymm
0	0.0 + 1.0	10000000	399953	27920	13556	0.04000	0.00415	2.06 ± 0.02
1	1.0 + 1.0	10000000	1628053	142211	36695	0.16281	0.01789	3.88 ± 0.02
2	2.0 + 1.0	10000000	2238223	232958	34691	0.22382	0.02676	6.72 ± 0.04
3	3.0 + 1.0	10000000	2048413	243893	22714	0.20484	0.02666	10.74 ± 0.07
4	4.0 + 1.0	10000000	1514708	200007	12707	0.15147	0.02127	15.74 ± 0.14
5	5.0 + 1.0	10000000	976912	140562	6133	0.09769	0.01467	22.92 ± 0.30
6	6.0 + 1.0	10000000	571885	88873	2854	0.05719	0.00917	31.14 ± 0.59
7	7.0 + 1.0	10000000	312163	51793	1287	0.03122	0.00531	40.24 ± 1.14
8	8.0 + 1.0	10000000	160819	28005	574	0.01608	0.00286	48.79 ± 2.06
9	9.0 + 1.0	10000000	79827	14595	228	0.00798	0.00148	64.01 ± 4.27
10	10.0 + 1.0	10000000	37923	7201	89	0.00379	0.00073	80.91 ± 8.63

qualitatively follow the energy spectrum of the sum of two neutron energies presented earlier in Fig. 4.1: it starts from about 0.4% asymmetry yield at 0 MeV point, reaches the maximum values of about 2.7% at the energy range of (3 - 4) MeV, and goes down up to 0.07% at 10 MeV point.

Also it would be interesting to calculate the two neutron asymmetry as a function of the energy cut on each neutron's energy and compare with the previous results. A such kind of calculation is presented in Fig. 4.4 and in table 4.2.

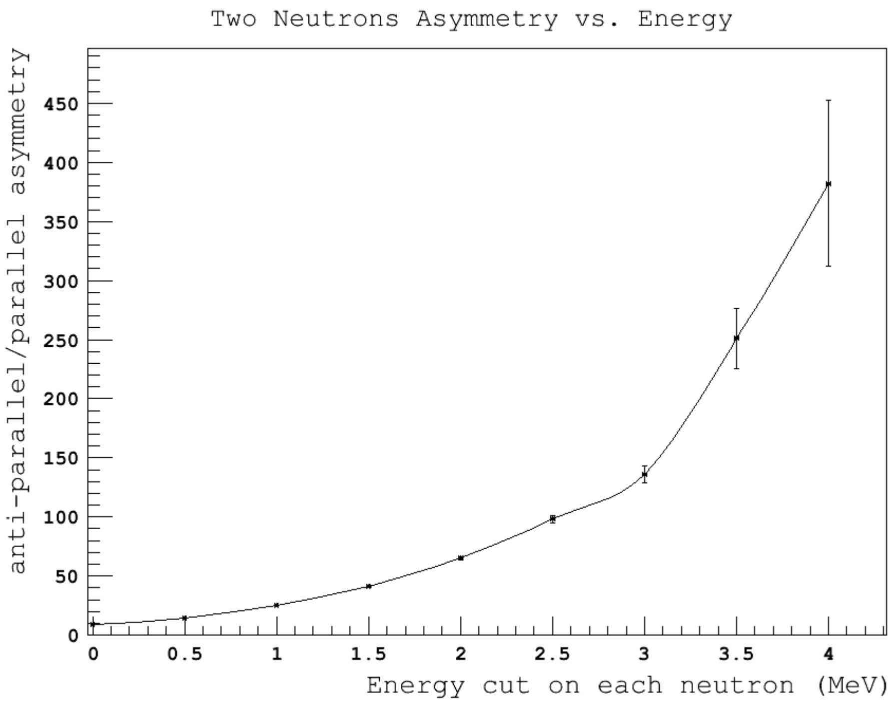

Figure 4.4: Calculated 2n asymmetry (antiparallel/parallel) as a function of the energy cut on each neutron energy

As we can see, by doing, say, 1 MeV energy cut on each neutron energy the expected asymmetry would be of about 25, and by doing 4 MeV energy cut the expected asymmetry reaches the huge value of about 380. Nevertheless, the problem here is as before: the number of counts at hight energy interval becomes smaller that will increase the error bars in expected asymmetry. It is interesting to note that even without any energy cut, by counting all neutron pairs going in antiparallel and in parallel directions, the expected asymmetry would be of about 9 and that corresponds to the maximum 2n asymmetry yield of about 13%.

In general, the results presented in table 4.2 is better then results presented in table 4.1 in the following sense. Foe example, in the first case (table 4.1), the maximum asymmetry yield we can get is about 2.7% and that corresponds to the 2n asymmetry value of about 10. In the second case, by doing, say, 0.5 MeV energy cut on each neutron energy, we can easily reach the asymmetry yield of about 10% and that will correspond to the 2n asymmetry value of about 15. By doing the energy cut we can significantly increase the calculated 2n asymmetry still having a good statistical error.

Table 4.2: Calculated 2n asymmetry (antiparallel/parallel) as a function of the energy cut on each neutron energy

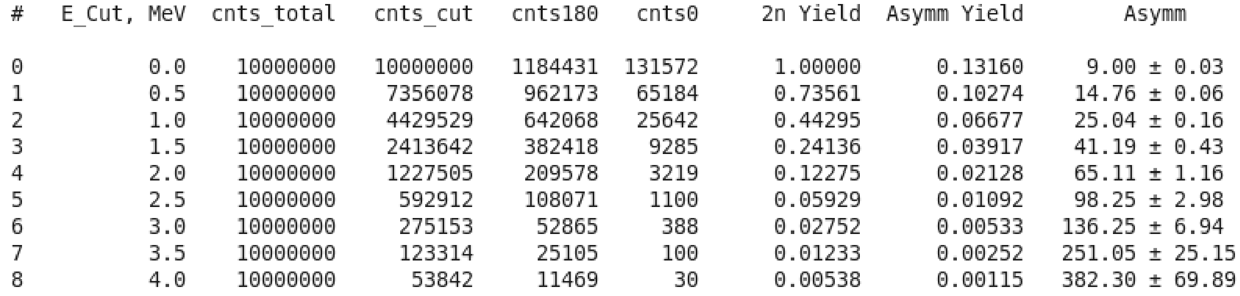

```
#   E_Cut, MeV  cnts_total   cnts_cut   cnts180   cnts0     2n Yield  Asymm Yield        Asymm

0         0.0    10000000   10000000   1184431  131572      1.00000      0.13160     9.00 ± 0.03
1         0.5    10000000    7356078    962173   65184      0.73561      0.10274    14.76 ± 0.06
2         1.0    10000000    4429529    642068   25642      0.44295      0.06677    25.04 ± 0.16
3         1.5    10000000    2413642    382418    9285      0.24136      0.03917    41.19 ± 0.43
4         2.0    10000000    1227505    209578    3219      0.12275      0.02128    65.11 ± 1.16
5         2.5    10000000     592912    108071    1100      0.05929      0.01092    98.25 ± 2.98
6         3.0    10000000     275153     52865     388      0.02752      0.00533   136.25 ± 6.94
7         3.5    10000000     123314     25105     100      0.01233      0.00252   251.05 ± 25.15
8         4.0    10000000      53842     11469      30      0.00538      0.00115   382.30 ± 69.89
```

There are several ways to make results discussed above more realistic. Some of them are directly following from the assumptions was made in simulation so far:

- we can use the more realistic FF's mass distribution (Fig. 1.3) instead of uniform one.
- we can use the more realistic multiplicity value instead of assumption that each fission fragment emits just one neutron.
- we can estimate the multiple Coulomb scattering effect inside the target. That, of course, will decrease the calculated 2n asymmetry results.

That all can be done later, however, the results of simulation show the huge asymmetry effect in 2n correlation. That will potentially permit a new technique for actinide detection for homeland security and safeguards applications.

4.2 Count rate calculation

It was shown in the previous sections that the expected 2n asymmetry (antiparallel/parallel) is a big number (f-la 1.7) and strongly depends from the sum of two neutron energies (fig. 4.3) as well as from the energy cut on each neutron (fig. 4.4). For example, we can expect the asymmetry value of about 65 doing 2 MeV cut on each neutron still having reasonable asymmetry yield of about 2%.

However, the problem arises as follow. Let assume we have N fission events per one beam pulse and let count how many two neutron coincidences are true and how many are accidental ones. The true coincidences are between two neutrons coming from the same fission event and obviously that for N fission events we will have N true coincidences. Let's call them $\mathrm{N_{true}}$. The accidental coincidences are between two neutrons but coming from the different fission events and, as can be easily seen, they are proportional to $N(N-1)$. Let call them $\mathrm{N_{accidental}}$. Now let calculate the following ratio:

$$\frac{\mathrm{N_{true}}}{\mathrm{N_{accidental}}+\mathrm{N_{true}}} = \frac{N}{N(N-1)+N} = \frac{1}{N} \tag{4.3}$$

To be able to observe the true coincidences we want the ratio above to be equal to one. The only way to do it is to make $N = 1$. That will guarantee that every coincidence will be a priory a true one with no way to have the accidental one. So we need to design the experiment in such way that the following condition is satisfied:

$$\mathrm{N} = \frac{\text{1 fission event}}{\text{pulse}} \tag{4.4}$$

Let's do the count rate calculation to check the possibility to satisfy to the condition above. By taking $\tau = 20\ ns$ pulse width and $I = 20\ mA$ peak current the number of electrons per pulse will be:

$$N_{e^-} = 20\cdot 10^{-3}\frac{\text{Coloumb}}{\text{sec}} \times \frac{1\ \mathrm{e}^-}{1.6\cdot 10^{-19}\ \text{Coloumb}} \times 20\ \text{ns} = 2.5\cdot 10^{9}\ \frac{\mathrm{e}^-}{\text{pulse}} \tag{4.5}$$

To be specific, let use the ^{235}U as a target. The figure 4.5 shows (γ, f) and $(\gamma, 2n)$ photo-nuclear cross sections as function of incident photon energy [25]. As can be seen, the optimal energy of incident gammas would be of about 6-7 MeV in the following sence. First, the (γ, f) cross section is low in this energy interval, doing possible to satisfy the desired condition of having one impulse per pulse. Second, there is no way to have the '2n knockout' because we well below the threshold energy of about 12 MeV for the $(\gamma, 2n)$ channel. By choosing, say, the 7 MeV electron beam energy, we will be able to study the pure (γ, f) channel.

The bremsstrahlung spectrum with 7 MeV endpoint energy for the thin Al radiator is shown in the figure 4.6. That will produce of about 0.05 photons/e$^-$/MeV/r.l. in the 6-7 MeV region.

Taking the thickness of Al radiator equal to 90 microns (about 10^{-3} radiation length), the number of bremsstrahlung photons going out of radiator in the 6-7 MeV energy range can be calculated as follow:

$$N_{\gamma'} = 2.5\cdot 10^{9}\ \frac{\mathrm{e}^-}{\text{pulse}} \times 0.05\ \frac{\text{photons}}{\mathrm{e}^-\ \text{MeV r.l.}} \times 1\ \text{MeV} \times 10^{-3}\ \text{r.l.} = 1.25\cdot 10^{5}\ \frac{\gamma'\text{s}}{\text{pulse}} \tag{4.6}$$

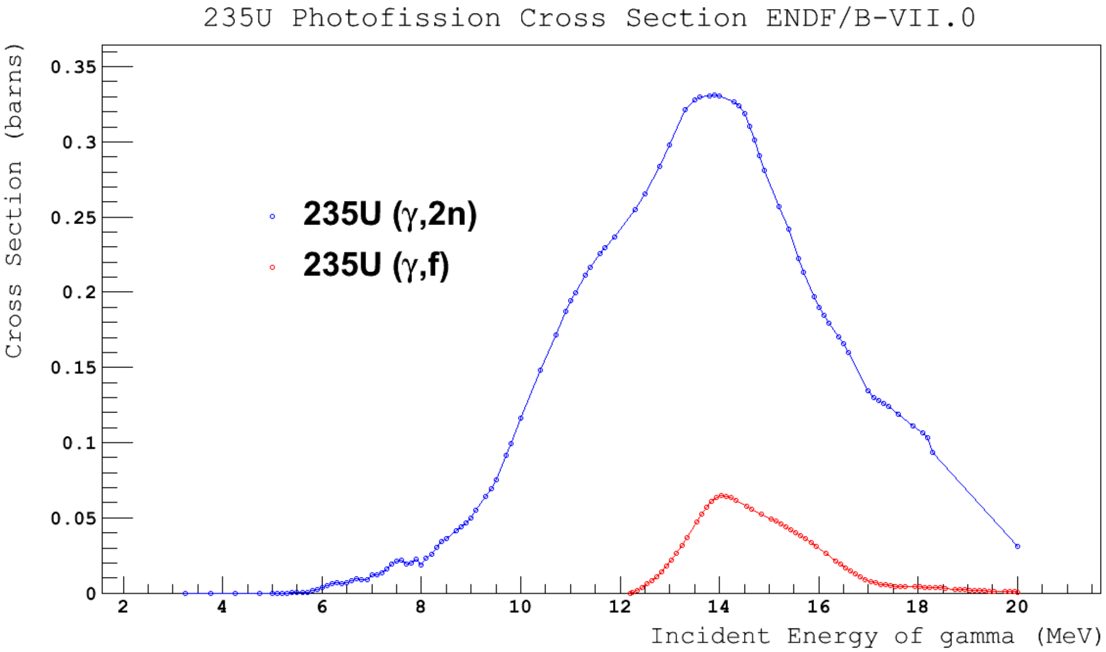

Figure 4.5: ^{235}U photofission cross section taken from ENDF/B-VII.0

Not all photons calculated above will hit the target. Some of them will be lost due to collimation. Assuming the collimation factor is about 50%, the number of photons hitting the target becomes:

$$N_\gamma = \mathrm{N}_{\gamma'} \times 50\% = 6.25 \cdot 10^4 \ \frac{\gamma'\mathrm{s}}{\mathrm{pulse}} \tag{4.7}$$

We want the one fission per pulse. That can be found by adjusting the target thickness from the equation below:

$$\frac{1 \text{ fission}}{\text{pulse}} = N_\gamma \times t \times \sigma \tag{4.8}$$

where t the is the target thickness in atoms/cm^2 and the σ is the $(\gamma, 2n)$ photo-nuclear cross section and is about 7 mb/atom in the 6-7 MeV energy range as can be seen from the figure 4.5 above. The thickness becomes:

$$\mathrm{t}\left[\frac{\mathrm{atoms}}{\mathrm{cm}^2}\right] = \frac{1\frac{\mathrm{fission}}{\mathrm{pulse}}}{6.25 \cdot 10^4 \ \frac{\gamma'\mathrm{s}}{\mathrm{pulse}} \times 7 \ \frac{\mathrm{mb}}{\mathrm{atom}}} = 2.29 \cdot 10^{21} \ \frac{\mathrm{atoms}}{\mathrm{cm}^2} \tag{4.9}$$

that could be converted into the cm as follow:

$$t\ [cm] = \frac{\mathrm{t} \cdot \mathrm{M}}{\rho \cdot \mathrm{N_A}} = \frac{2.29 \cdot 10^{21} \ \frac{\mathrm{atoms}}{\mathrm{cm}^2} \times 235.04 \ \frac{\mathrm{g}}{\mathrm{mol}}}{19.1 \ \frac{\mathrm{g}}{\mathrm{cm}^3} \times 6.02 \cdot 10^{23} \ \frac{\mathrm{atoms}}{\mathrm{mol}}} = 470 \ \mu\mathrm{m} \tag{4.10}$$

where M is the molar mass, ρ is the density of ^{235}U and N_A is the Avogadro number.

In the last step we was able by varying the target thickness to satisfy the desired situation of having the one fission per pulse. In principal, the other elements of the beam line, like

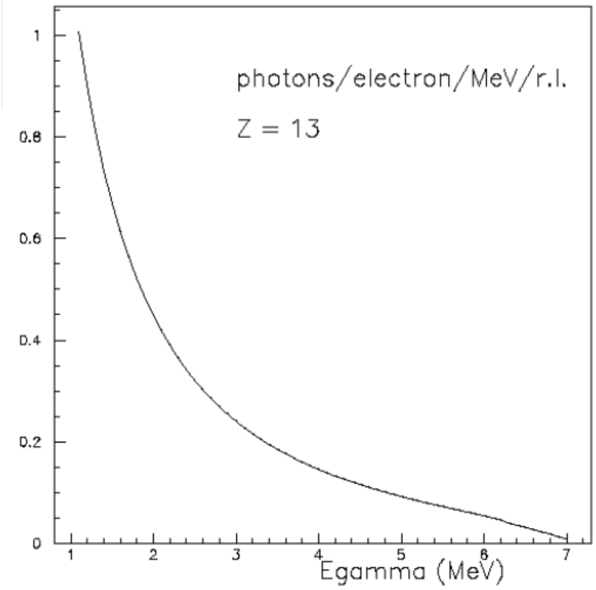

Figure 4.6: Bremsstrahlung spectrum of photons produced by 7 MeV electrons hitting the Al radiator

thickness of the radiator or the collimation hole, can be varied as well. After the reasonable judgment about the beam line elements is done, we still have the possibility to adjust the count rates by varying the LINAC beam parameters, such as the electron pulse width and the electron peak current.

4.3 Beam time calculation

Let's now estimate the time needed to run the experiment. As was already mentioned in the previous section to eliminate the accidental coincidence the one fission per pulse rate is required and because that the Hight Repetition Rate Linac (HRRL) available at IAC will be a good choice.

Let's calculate the coincidence rate we would expect for two neutron detectors located 2 m away from the target as presented in Fig 4.7.

The count rate for both detectors can be calculated as:

$$\mathrm{N}\ \left[\frac{\mathrm{coinc}}{\mathrm{sec}}\right] = \frac{1\ \mathrm{fission}}{\mathrm{pulse}} \cdot \mathrm{N}_{\mathrm{G}}^2 \cdot \mathrm{N}_{\mathrm{intr}}^2 \cdot \mathrm{N}_{\mathrm{cut}} \cdot 2.2 \cdot 10^3\ \mathrm{Hz} \tag{4.11}$$

where N_{G} is the geometrical detector efficiency, $\mathrm{N}_{\mathrm{intr}}$ is the absolute intrinsic detector efficiency, $\mathrm{N}_{\mathrm{cut}}$ is the efficiency of the energy cut, 2.2 is the average number of neutrons per fission, 10^3 Hz is the HRRL repetition rate.

The geometrical detector efficiency N_{G} is just the solid angle as the target see the detector and can be calculated as following:

$$\Omega = \frac{\mathrm{S}}{4\pi \mathrm{r}^2} = \frac{(15 \times 88)\ \mathrm{cm}^2}{4\pi(2\ \mathrm{m})^2} = \frac{0.132\ \mathrm{m}^2}{50.258\ \mathrm{m}^2} = 2.6 \cdot 10^{-3}\ \mathrm{sr} \tag{4.12}$$

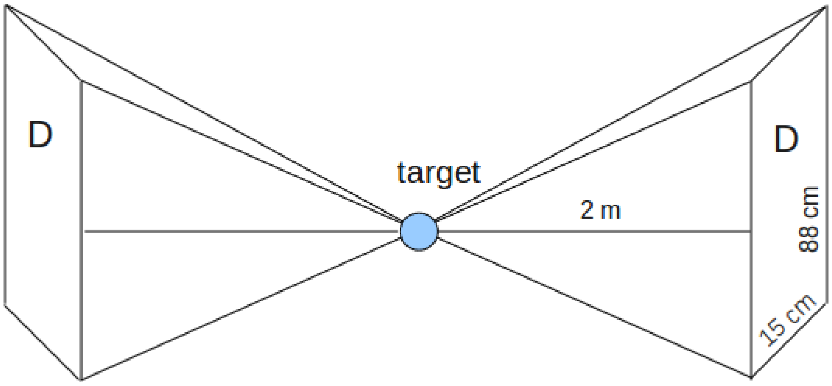

Figure 4.7: Two detector geometry located 2 m away from target

.

The intrinsic detector efficiency N_{intr} can be conservatively assumed to be about 25%. The efficiency of energy cut N_{cut} can be estimated from table 4.2 and for 1 MeV energy cut is about 44%. Substituting all values above in the formula 4.11 the counts rate for two detectors becomes:

$$N = \frac{1\ \text{fission}}{\text{pulse}} \cdot (2.6 \cdot 10^{-3})^2 \cdot (0.25)^2 \cdot 0.44 \cdot 2.2 \cdot 10^3\ \text{Hz} = 4 \cdot 10^{-4}\ \frac{\text{coinc}}{\text{sec}} \tag{4.13}$$

There are total 16 neutron detectors available for that experiment that will increase the count rate by the factor of $8 \times 8 = 64$ so the count rate for 16 detectors becomes:

$$N_{16\ \mathrm{det}} = N \times 64 = 2.6 \times 10^{-2}\ \frac{\text{coinc}}{\text{sec}} \tag{4.14}$$

The expected statistics for 1 working day of the beam time (8 hours) will be:

$$N_{\mathrm{day}} = N_{16\ \mathrm{det}} \times 60\ \text{sec} \times 60\ \text{min} \times 8\ \text{hours} \approx 750\ \frac{\text{coinc}}{\text{day}} \tag{4.15}$$

that is good enough to analyze the experimental data.

Chapter 5

Summary, conclusion

Below are the short summary and conclusion of proposed here two neutron correlation study:

- There are needs in experimental data of two neutron correlation measurements in fission.
- The preliminary calculation of the two neutron correlation shows a huge asymmetry effect: much more neutrons are emitted anti-parallel to each other than parallel to each other. That asymmetry becomes even more if the energy cut on each neutron is done. There are some factors, as multiple Coulomb scattering, for example, that will reduce the calculated asymmetry and that could be calculated later. But that will not reduce the expected asymmetry significantly.
- We propose to measure and analyze the two neutron correlation yield resulting from two FF's as a function of different targets, the angle between the two neutrons and the neutron energies by utilizing well developed at IAC the bremsstrahlung photons production techniques. There are total 16 'big' plastic detectors available at the present time, which can be used for neutron detection. With High Repetition Rate Linac we can get of about 750 coincidences per day.
- This study will potentially permit a new technique for actinide detection for homeland security and safeguards applications as well as improve our knowledge of correlated neutron emission.

Bibliography

[1] K.S. Krane, *IBntroductory Nuclear Physics*, John Wiley & Sons, Inc., New York, 1988.

[2] S.S.M. Wong, *Introductory Nuclear Physics*, John Wiley & Sons, Inc., New York, 1988.

[3] V.Weisskopf, *"Statistics and Nuclear Reactions"*, Phys. Rev. **52**, 295 (1937).

[4] M.Goldhaber and E.Teller, *"On Nuclear Dipole Vibrations"*, Phys. Rev. **74**, 1046–1049 (1948).

[5] A.Bohr, *On the theory of nuclear fission*, Proc. 1st UN Int. Conf. on peaceful uses of atomic energy, Vol 2, 151, New York 1956.

[6] E.J.Winhold, P.T.Demos, and I.Halpern, Phys. Rev. **85**, 728(A) (1952)

[7] E.J.Winhold, P.T.Demos, and I.Halpern, *"The Angular Distribution of Fission Fragments in the Photofission of Thorium"*, Phys. Rev. **87**, 1139–1140 (1952)

[8] A.W.Fairhall, I.Halpern, and E.J.Winhold, *"Angular Anisotropy of Specific Thorium Photofission Fragments"*, Phys. Rev. **94**, 733–734 (1954)

[9] E.J.Winhold and I.Halpern, *"Anisotropic Photofission"*, Phys. Rev. **103**, 990–1000 (1956)

[10] H.R. Bowman, S.G. Thompson, J.C.D. Milton, and W.J. Swiatecki, *Velocity and Angular Distributions of Prompt Neutrons from Spontaneous Fission of* Cf^{252}, Phys. Rev., **126**, 2120 (1962).

[11] R. Ratzek, W. Wilke, J. Drexler, R. Fischer, R. Heil, K. Huber, U. Kneissl, H. Ries, H. Ströher and R. Stock, et al., *Photofission with linearly polarized photons* , Z.Phys.A - Atom and Nuclei **308**, 63 (1982).

[12] C.Budtz-Jorgensen and H.-H.Knitter, *Simultaneous investigation of fission fragments and neutrons in* ^{252}Cf *(SF)*, Nucl. Phys. **A490**, 307 (1988).

[13] U.E.P. Berg and U. Kneissl, Ann. Rev. Nucl. Part. Sci. **37**, 33-69 (1987).

[14] A. De Clercq, E. Jacobs, D. De Frenne, H. Thierens, P. D'hondt, and A. J. Deruytter, *Fragment mass and kinetic energy distribution for the photofission of* ^{235}U *and* ^{238}U *with 25-MeV end-point bremsstrahlung*, Phys. Rev. C **13**, 1536 (1976).

[15] E.Jacobs, A.De Clercq, H.Thierens, D.De Frenne, P.D'hondt, P.De Gelder, and A.J.Deruytter. *Fragment mass and kinetic energy distributions for the photofission of* ^{235}U *with 12-, 15-, 20-, 30-, and 70-MeV bremsstrahlung*, Phys. Rev. C **24**, 1795–1798 (1981)

[16] W.Wilke, U.Kneissl, Th.Weber and all., *Photofission of* ^{238}U *with monochromatic gamma rays in the energy range 11–16 MeV*, Phys. Rev. C **42**, 2148–2156 (1990)

[17] Talou, P. and Becker, B. and Kawano, T. and Chadwick, M. B. and Danon, Y. *Advanced Monte Carlo modeling of prompt fission neutrons for thermal and fast neutron-induced fission reactions on* ^{239}Pu, Phys. Rev. C, **83**, 064612 (2011).

[18] V. F. Apalin, Yu.N. Gritsyuk, I. E. Kutikov, V. I. Lebedev, and L. A. Mikaelian, Nucl. Phys. **71**, 553 (1965).

[19] C.Wagemans, E.Allaert, A.Deruytter, R.Barthélémy, and P.Schillebeeckx, *Comparison of the energy and mass characteristics of the* $^{239}Pu(n_{th}, f)$ *and the* $^{240}Pu(sf)$ *fragments*, Phys. Rev. C **30**, 218 (1984).

[20] V.M.Surin, A.I.Sergachev, N.I.Rezchikov, B.D.Kuz'minov *"Yields and kinetic energies of fragments in the fission of U233 and Pu239 by 5.5- and 15-MeV neutrons"*, Yad. Fiz. **14**, 935 (1971).

[21] C.Tsuchiya, Y.Nakagome, H.Yamana, H.Moriyama, K.Nishio, I.Kanno, K.Shin, and I.Kimura, *"Simultaneous Measurement of Prompt Neutrons and Fission Fragments for* $^{239}Pu(n_{th}, f)$*"*, J. Nucl. Sci. Technol. **37**, 941 (2000).

[22] M.Asghar, F.Caitucoli, P.Perrin, and C.Wagemans, *"Fission fragment energy correlation measurements for the thermal neutron fission of* ^{239}Pu *and* ^{235}U*"*, Nucl. Phys. A **311**, 205 (1978).

[23] P.Talou, T.Kawano, O.Bouland, J.E.Lynn, P.Möller, and M.B.Chadwick Proceedings of the International Conference on Nuclear Data for Science & Technology ND2010, April 26–30, 2010, Jeju Island, Korea.

[24] K.-H. Schmidt and B. Jurado. *"Entropy Driven Excitation Energy Sorting in Superfluid Fission Dynamics"*, Phys. Rev. Lett. **104**, 212501 (2010).

[25] *National Nuclear Data Center*, http://www.nndc.bnl.gov/